Type of contribution:
Editorial
▶ Research Paper
Case Study
Review Paper
Scientific Data
Report of Tech. Application

mesi e-issn. 2798-5245

Mechanical Engineering for Society and Industry
Vol. 5, No. 2 (2025) pp 459-479
https://doi.org/10.31603/mesi.14096

Optimization air circulation in negative pressure closed-house poultry buildings: A study on evaporative cooling pad thickness and exhaust fan operating pattern

Zain Lillahulhaq[1], Wawan Aries Widodo[1]*, Sutardi[1], Thearith Yone[2]

[1] Department of Mechanical Engineering, Sepuluh Nopember Institute of Technology (ITS), Surabaya 60117, **Indonesia**
[2] Department of Mechanical Engineering, Royal University of Phnom Penh, Phnom Penh 120404, **Cambodia**
✉ wawanaries@its.ac.id

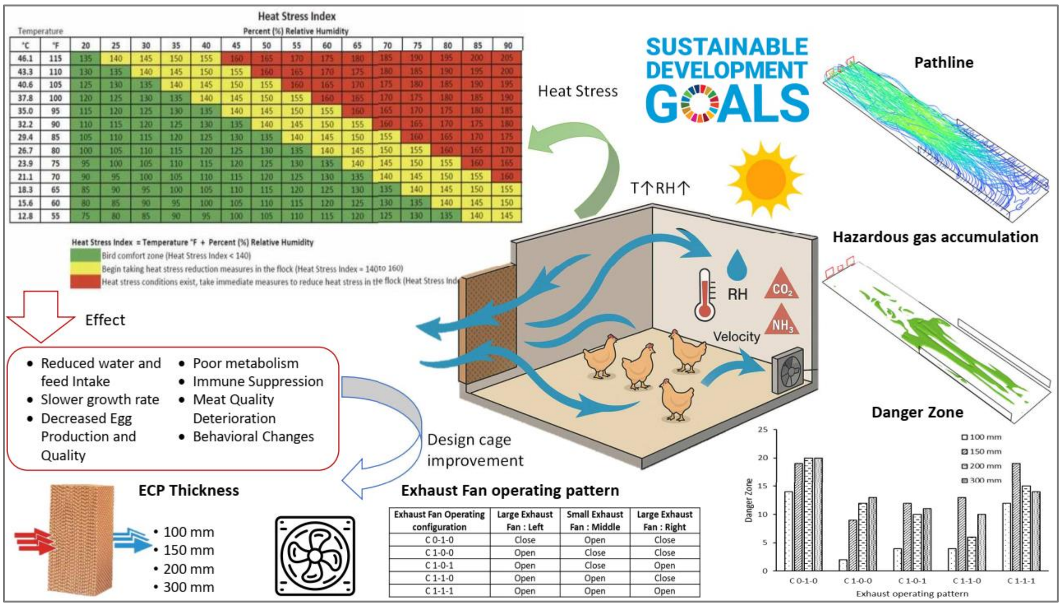

Highlights:

- The close-house cage employs a negative pressure ventilation system to sustain optimal conditions for poultry. Variations in ECP thickness and exhaust fan configurations lead to distinct distributions of dead zones and damaging zones.
- The distribution of temperature, relative humidity, airflow, and dangerous gases like CO_2 and NH_3 are shown numerically in simulations of the close-house cage. The 100 mm ECP created the fewest dangerous zones. The placement of evaporative cooling pads (ECPs) raised humidity and decreased temperature.
- Multiple exhaust fan operation successfully eliminated heat stress zones. Full exhaust fan operation (C 1-1-1) increased dangerous zones due to hazardous gas accumulation, despite higher airflow.
- Thinner ECPs combined with optimized exhaust fan patterns improved thermal comfort and air quality in close-house cages.
- The C 1-1-0 is optimum configuration pattern which has minimum hazardous area inside close-house cage

Article info
Submitted: 2025-07-09
Revised: 2025-11-08
Accepted: 2025-12-28

Publisher
Universitas Muhammadiyah Magelang

Abstract

An optimal environment for raising poultry requires a cool, humid climate. Negative pressure air circulation is widely implemented in closed-house cages, combined with evaporative cooling pads (ECP). Fresh air cannot naturally pass through the ECP due to the porosity of the material. The characteristics of the ECP and the configuration of the exhaust fan operating pattern affect airflow distribution, including velocity, temperature, and relative humidity (RH) levels. This research simulated the effect of varying ECP thickness on airflow distribution inside a closed-house cage.

The simulation was run under 3D steady-state conditions with ECP thicknesses of 100 mm, 150 mm, 200 mm, and 300 mm, respectively. The ECP was kept wet, resulting in incoming air with 60% humidity and a temperature of 27 °C. The study used the K-ω SST turbulence model and SIMPLE second-order discretization. The analysis also provides recommendations for optimal exhaust fan operation during summer and identified restricted area. Five different fan operating patterns were tested, combining a small exhaust fan with two large ones. This analysis based on several parameter which refers uncomfortable environment, including: velocity, temperature, RH levels, and pollutant gas concentration. Hazardous conditions were determined by the maximum values observed across 42 iso-surfaces spaced 1 meter apart along the x-axis. A thicker ECP resulted in a higher pressure drop, reducing temperature differences inside the cage and leading to a more uniform temperature distribution. The 100 mm ECP thickness, the thinnest ECP layers, lowered the temperature inside the closed-house cage. The study suggests that, during summer, operating one small exhaust fan and one large fan is optimal due to the reduced presence of hazardous areas inside the cage.

Keywords: Poultry; Negative pressure air circulation; Closed-house cages; Evaporative cooling pads; Exhaust fan operating patterns

1. Introduction

The closed-house cage poultry system is an intensification program aimed at enhancing livestock productivity. The ventilation in close house cage is equipped with a mechanical air circulation system, such as standard fans or exhaust fans. Air circulation in closed-house cages is classified into positive and negative pressure based on the ventilation system [1]. In a positive pressure ventilation system, standard fans used to push fresh air into the room. Otherwise, negative pressure ventilation relies on the pressure difference between the ambient air inside the cage and the atmospheric pressure outside. The ambient pressure inside the closed-house cage is lower than the atmospheric pressure due to the suction effect generated by exhaust fans. Positive pressure ventilation effectively prevents contaminated air from entering the room. Whereas negative pressure ventilation is effective in reducing the spread of airborne pathogens such as mold, dust, viruses, and indoor pollution. Negative pressure air circulation is widely implemented in closed-house cages [2], [3], [4], [5], [6], [7], respectively. Though it consumes more electricity. Nowdays, negative pressure air circulation in closed-house cages is combined with evaporative cooling pads (ECPs) [8], [9], [10]. ECPs serve as filters, preventing insects from invading the close house cage. These pads are made from chemically reinforced cellulose, designed with specific angles and porosity to ensure uniform airflow [11]. The porosity of ECPs resulted pressure drop in air supply as it passes through [12].

Fresh Air cannot naturally pass through the ECP due to the porosity of material. It necessary to add some equipment to gain higher pressure to supply fresh air into the closed-house cage. ECPs Instalment are combined with exhaust fans to create a suction effect on fresh air to prevent heat stress in poultry. Heat stress occurs when high temperatures and humidity inside the close house obstruct the chicken's ability to dissipate heat. Heat stress potentially interrupt chicken metabolism system and causing sudden death [13]. This condition also causes inconvenience, a high mortality rate for birds, a weak immune response, and low productivity. In laying hens, the production is decreased in egg weight and quality, where it has thin and breakable eggshell [14].

Prevention of heat stress effect involves regulation of temperature and humidity level inside the cage. In hot and dry weather, ECPs are moistened by pumped water to enhance room humidity [15]. Farmers must fulfil several criteria to mitigate heat stress in the poultry. First, the airflow pattern inside the closed-house cage must have uniform humidity, temperature, and velocity. Second, air pollutants from chicken metabolism must be expelled from the cage rapidly. Innovations through experimental and numerical studies have aimed to create uniform airflow patterns while reducing the energy consumption of exhaust fans and pumps. Experimental research has focused on enhancing performance and efficiency [12], cooling capacity [5], [16], and pressure drop through various improvements, such as adjustments on the angle of inlet angles [17], water consumption [15], [18], porosity [19], [20], materials [21], and type ECP installation systems [22]. However, these studies are typically conducted on a laboratory scale and may not be directly applicable to actual closed-house cages. Numerical simulations offer a valuable alternative on studying the effects of ECP installation in closed-house cages. Numerical simulation is an efficient method to illustrate the air flow pattern and thermal distribution especially time and cost [23], [24]. The simulation also avoids the direct animal involvement, thereby reducing livestock stress. Numerical simulations provide detailed insights into temperature, airflow velocity, and particle distribution at various points. It also has precise prediction on the airflow patterns based on seasonal and weather conditions [25].

A numerical simulation was conducted to assess the impact of distances between the Evaporative Cooling Pad (ECP) and the rear side of the closed house. The Distances considered were varied on 0, 2, 3, and 4 meters, respectively. The simulation, performed under steady-state conditions using the standard k-ε turbulence model [26]. The closed-house cage design is simplified into a cube. The ECP described as the inlet and the exhaust fan as the outlet. The result shows that it is crucial to maintain an optimal distance between the ECP and the rear wall to prevent excessive cooling. Another study explored the effects of different ECP installation positions on airflow patterns inside the closed-house cage [27], [28]. The Exhaust fan is located on: Model A at the front of the cage, Model B at the rear cage, and Model C on the sidewall of the cage. This simulation employed a 3D steady-state model using the K-epsilon RNG (Renormalization Group) turbulence method. The ECP is modelled as the inlet velocity and the exhaust fan as the pressure [27]. Post-processing of simulation result provided vector and contour of airflow distribution. These results can be further analyzed using statistical methods, such as ANOVA or the Hosmer-Lemeshow test. A further analysis can determine the primary factors influencing airflow distribution inside the closed house, including incoming air velocity, diffuser placement, window height [29], aspect ratio and inlets positioning [30].

Indonesian farmers receive some investments from livestock companies in the form of funds, DOC (Day-Old Chicks), feed, and cages, and later sell the livestock back to the company at harvest time. The companies also provide farmers with a closed-house cage design and an HVAC system. However, the operation of exhaust fans relies more on farmer's intuition and practical experience rather than a consideration of air distribution inside the cage. This study aimed to assess the impact of varying exhaust fan operating patterns in a basic closed-house cage. Several assumptions were implemented in this study in order to get closer representation with actual conditions. The closed-house cage was equipped with an evaporative cooling pad on the sidewall. Unlike previous studies [25], [31] this research concentrated on airflow distribution changes due to the pressure drop effect caused by the ECP. This study was conducted using 3D numerical methods under steady flow conditions. The findings are expected to produce recommendations on optimal operating patterns and on the influence of evaporative cooling pad (ECP) thickness on airflow distribution within closed-house cages under summer conditions. These recommendations are derived from simulation-based mapping of heat-stress risk regions and airflow dead zones. With this evidence, farmers can reduce mortality by optimizing air-circulation management.

1.1. Geometry

This study was designed to evaluate the air distribution pattern of a closed-house cage. The cage's ventilation system operates under negative pressure, utilizing two large exhaust fans and one smaller fan. The openings of the closed-house cage are fitted with covers that can be manually adjusted by the farmer when not in operating mode. Additionally, the cage is equipped with Evaporative Cooling Pads (ECP) on both sides of the inlets. During the summer, Water pumps are activated by farmers to dampen the ECP walls during the summer to increase humidity level inside the cage. The cage walls are insulated to prevent external heat from penetrating directly. The close house cage has length x width x height: 42 x 8 x 2 m with 2.7 m^2 ECP each side. The geometric dimensions of the closed-house cage are provided in **Figure 1**.

The first stage of this study is to investigate the effect of exhaust fan operating configuration. This study investigated the effects of varying exhaust fan operation patterns, as detailed **in Table 1**. The ECP was maintained in a wet condition, resulting in incoming air with 60% humidity and a temperature of 27 °C [2]. To reflect actual conditions, the simulation utilized an ECP with a thickness of 200 mm. The heat source in the simulation came from the chickens 46.6 w/m^3 [32]. The boundary conditions applied in this study are outlined in **Table 2**.

Table 1. Configuration of exhaust fan operating pattern

Exhaust Fan Operating configuration	Large Exhaust Fan: Left	Small Exhaust Fan: Middle	Large Exhaust Fan: Right
C 0-1-0	Close	Open	Close
C 1-0-0	Open	Close	Close
C 1-0-1	Open	Close	Open
C 1-1-0	Open	Open	Close
C 1-1-1	Open	Open	Open

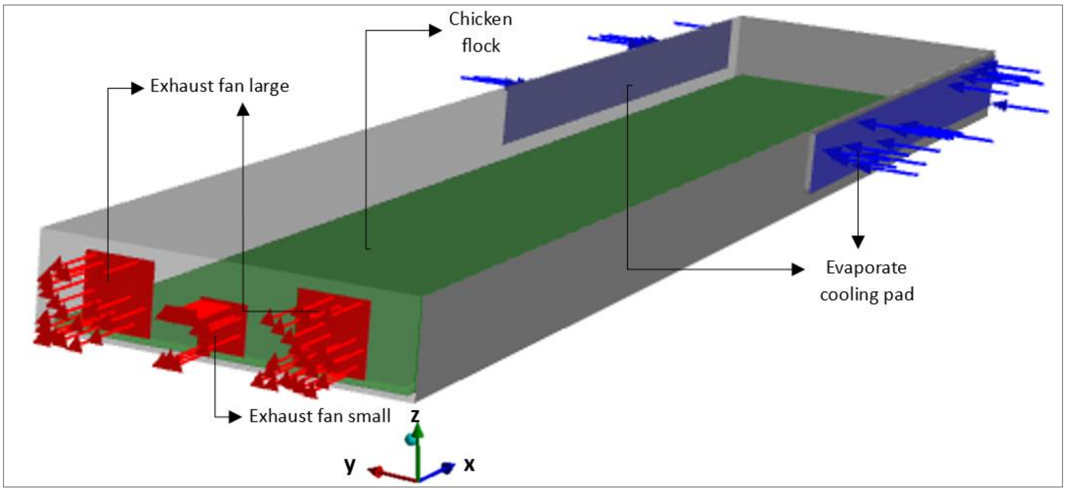

Figure 1. The dimensions of the closed-house cage

Table 2. Boundary condition in the simulation

	Boundary
Evaporate cooling pad	Pressure inlet
Exhaust fan	Pressure Out
Wall	Adiabatic Wall
Chicken	Wall heat flux

Afterward, the simulation was run to investigate the effect of ECP thickness on close house cage. The 3D steady condition was simulated with ECP thicknesses of 100, 150, 200, and 300 mm, respectively. The set up of porosity is calculate in the next section.

1.2. Porosity Set Up

The airflow entering the closed-house cage should maintain uniform velocity due to its passage through the evaporative cooling pad (ECP). The ECP installation induces a pressure drop effect on the airflow distribution. This study evaluate the pressure drop effect of the ECP based on the porosity-porous medium equation. To assess the pressure drop precisely, it is essential to calculate the porous media characteristic based on inlet velocity. The different thickness of ECP has specific pressure drop due the viscous and inertial resistance value. The calculations can be performed using the following equation:

$$-\frac{\Delta P}{l} = \frac{\mu}{K_f}V + \beta\rho V^2 \qquad (1)$$

ΔP denotes the specific pressure drop (Pa), derived from V, which indicates velocity (m/s), and ℓ represents the ECP thickness (m). μ represent fluid viscosity (N.s/m²). This equation is applicable for high Reynolds number flows, where Kf denotes Forchheimer's permeability (m²), ρ represents fluid density (kg/m³), and β is a dimensionless number. This equation is commonly used in studies of ECP pressure drop [25], [33], [34], [35], [36]. In addition to the quadratic formulation, the pressure drop can also be described by the cubic law, where γ is the inertial factor [17]. However, the cubic law equation tends to have greater error compared to the quadratic pressure drop equation [17], [37].

$$-\frac{\Delta P}{l} = \frac{\mu}{K_f}V + \frac{\gamma}{\mu}\rho^2 V^3 \qquad (2)$$

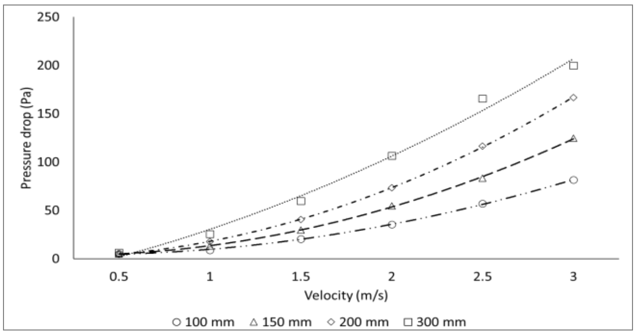

Figure 2. Pressure drop across different evaporative cooling pad thicknesses as a function of velocity

In research conducted by Franco [17], the use of the cubic law equation did not provide a higher accuracy in pressure drop value than the quadratic equation. Therefore, in this study, the quadratic equation is applied. This study was conducted on close house cage with ECP thicknesses of 100, 150, 200, and 300 mm, respectively. The pressure drop–velocity values were obtained from Lakzini's research [12] Based on the calculations using the Eq. (1), the viscous resistance and inert resistance constants were obtained as follows **Figure 2** and **Table 3**.

Table 3. The value of viscous and inertial resistance in various ECP

ECP thickness	Viscous resistance	Inertial resistance
100 mm	2693460.03	83.37
150 mm	2141382.52	82.99
200 mm	657993.290	78.6
300 mm	7097261.04	34.1

1.3. Turbulence Model

The choice of turbulence model is crucial in determining the accuracy of numerical simulations. The K-ε turbulence model is commonly used in the other literature to analyze indoor airflow and environmental parameters for livestock. However, the realizable K-ε turbulence model offers enhancements in predicting flow rotation, recirculation, and boundary separation [36], [38]. In that study, the RNG K-ε turbulence model was employed to assess turbulent effects which combine with Discrete Ordinates (DO) radiation to estimate radiation heat transfer [31].

Previous research involved a numerical simulation of a closed-house cage with one large exhaust fan and one small exhaust fan. In that study, the turbulence model was validated by measuring room temperature and velocity at various points. The K-ω SST turbulence model effectively captured changes in temperature and airflow velocity inside the closed-house cage. Nevertheless, the RNG K-ε turbulence model provided a more accurate prediction of airflow velocity, though it was less precise in predicting temperature changes. Therefore, this study applies the K-ω SST turbulence model due to its closer alignment with actual temperature and velocity measurements.

The expected results of this study include identifying vortex areas created by airflow inside the closed-house cage. Thus the research utilized a discretization Navier-Stokes system model with velocity-pressure coupling equations. The turbulence intensity applied was 3.25% [39], and the simulations used second-order equations with the Semi-Implicit Method for Pressure-Linked Equations (SIMPLE).

1.4. Post-Processing

Post-processing is a crucial step to illustrated simulation result into comperhensif and comunicative data. This study is illustrated flow distribution through variations in velocity contours, relative humidity, temperature, and the distribution of hazardous gases (CO_2 and NH_3). The velocity of air distribution is illustrated through pathlines to emphasize vortex transformations. Humidity and temperature contours are captured at y/h = 0.25 m, corresponding to the height of a chicken's head. The accumulation of hazardous gases is visualized using 3D iso-surface contours. Besides the Hazardous gases accumulation, Damaging and dead zone are also presented to indetified the areas where farmers should highly avoid to minimize mortality. A region with minimal fluid velocity, known as a dead zone, may develop ahead of the ECP. The damaging zone is defined by high-velocity regions that might appear in nearby of the exhaust fan [40], [41]. In this paper, the dead and damaging zones are defined more properly, without presuming the location from the evaporative cooling pad (ECP) or the exhaust. A dead zone is an area of low air velocity surrounded by air moving at higher velocities; therefore, a dead zone is not necessarily located upstream of the ECP. In contrast, a damaging zone is an area within the closed-house cage where the local air velocity exceeds that of the immediately surrounding flow [38]. Minimizing the dead zones and damaging zones is crucial to reducing negative effects on the livestock. These negative effects can result from the accumulation of harmful gases, such as NH_3 and CO_2, or exposure to high-velocity fluid flows. Beyond contour representations, the airflow distribution inside the closed-house cage is further explained by presenting graphs of the average isosurface values along the x-direction. The analysis covers velocity, relative humidity (RH), and temperature distributions.

Furthermore, this study offers optimal recommendations for exhaust fan operation scenarios that farmers can adopt during the summer. The ideal exhaust fan operation pattern is characterized by the fewest restricted areas inside the closed house cage. The restricted areas is determined by the maximum value of 42 iso-surfaces along x direction, which distanced by 1 meter apart. The classification of the restricted area was carried out based on several parameters referring to an uncomfortable environment for poultry, such as hazardous gas accumulation (CO_2 and NH_3 levels), temperature, relative humidity (RH), and air velocity. The uncomfortable condition is basic criteria for defining hazardous areas in this study, wich shown in **Table 4**.

Table 4. The ideal criteria for poultry environment

Indicator	Limit
Air velocity	< 2 m/s
Temperature	293< T <298 K
Relative humidity	40< RH <60 %
CO_2	< 1000 ppm
NH_3	< 50 ppm

2. Results and Discussion

This research aims to evaluate the influence of ECP thickness variations and exhaust fan operating patterns. The initial phase involved installing ECPs with thicknesses of 100, 150, 200, and

300 mm under the C 1-1-0 operating pattern. In the subsequent phase, a 200 mm ECP was used to assess the effects of five different exhaust fan operating patterns. The results are presented through qualitative and quantitative analyses. Qualitative data include pathlines and contours of temperature, relative humidity (RH), and hazardous gas concentrations, while quantitative data are presented in graphical form. A final analysis is provided through a graph depicting the total dangerous zone.

2.1. Morphology Airflow Inside Close House Cage

Overall, the fluid flow within the closed-house cage exhibits a largely consistent morphology. The morphology shown in **Figure 3**. Incoming fluid flow through the ECP units collides as a result of their opposing arrangement. This collision generates two large vortices that swirl toward the exhaust fan. These vortices rotate at higher velocities due to the absence of friction with the walls. The centerline region serves as the convergence point of the two major vortices, and the fluid flow along the centerline demonstrates distinct characteristics compared to the vortex flow. Additionally, the fluid flow adjacent to the side walls experiences friction against the wall surfaces. The velocity near the side walls tends to be lower, not only due to friction but also because the sidewall flow is compressed by the larger vortices.

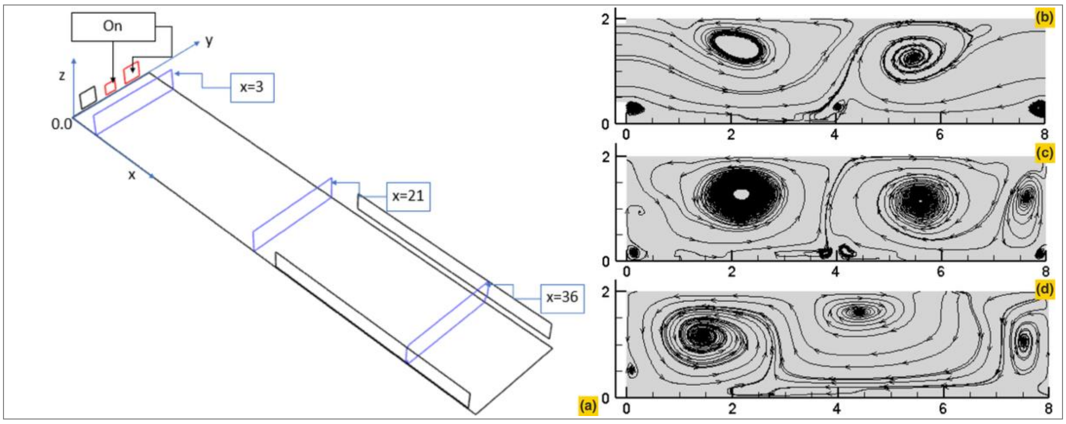

Figure 3. (a) Iso-surface visualization of airflow in a closed-house cage x = (b) 36; (c)21; (d) 3

2.2. The Effect of ECP Thickness

The simulation depicts the airflow distribution within the closed-house cage equipped with evaporative cooling pads (ECPs), operating both a large and a small exhaust fan. **Figure 4** presents the graph of maximum velocity values extracted from the isosurface along the x-axis. This simulation was conducted to examine the influence of evaporative cooling pad installation on airflow characteristics within the closed-house cage. The ECPs utilized had thicknesses of 100 mm, 150 mm, 200 mm, and 300 mm. Overall, all thickness variations exhibited a similar velocity trendline. The air entering through the evaporative cooling pads displayed low initial velocities, followed by an increase as the airflow approached the exhaust fans located at the front of the cage. The average air velocity within the closed-house cage exceeded 1.5 m/s across all ECP thickness variations, a value considered low and below the hazardous threshold for poultry. The ECPs with thicknesses of 100 mm and 150 mm resulted in comparable average velocities, while the airflow through the 200 mm and 300 mm ECPs demonstrated a similar velocity profile along the x-axis. The consistency of the average velocity trendlines suggests that variations in ECP thickness yield similar velocity distributions under identical operating conditions. More detailed distinctions in airflow distribution are illustrated through the pathline visualization.

The characteristics of fluid flow entering the closed-house cage are illustrated through the flow pathlines depicted in **Figure 5**. These pathlines demonstrate the interaction of airflow within the closed-house cage configured with both a small and a large exhaust fan in operation. The flow visualization highlights changes in fluid distribution following passage through evaporative cooling pads (ECPs) with thicknesses of 100 mm, 150 mm, 200 mm, and 300 mm.

The airflow entering through the ECPs exhibits reduced velocity due to a pressure drop induced by the material's porosity. The pressure drop increases as the thickness of the installed evaporative cooling pad (ECP) increases. Opposing streams from the facing ECPs collide and roll, forming vortices. The airflow at the center of the closed-house cage exhibits a reduction in momentum due to the collision. The velocity increases as the air moves toward the exhaust fan, whereas the air velocity near the side walls decreases due to frictional effects. In the center region of the closed-house cage, airflow velocity increases as the swirling motion propels the air toward the operating exhaust fan.

An increase in ECP thickness leads to a reduction in internal airflow velocity. As the ECP thickness increases, the vortices become larger, while the overall velocity diminishes. High-velocity airflow, marked by green coloration, is more frequently observed with thinner ECP installations, indicating that higher air velocities are achieved in closed-house cages fitted with thinner evaporative cooling pads.

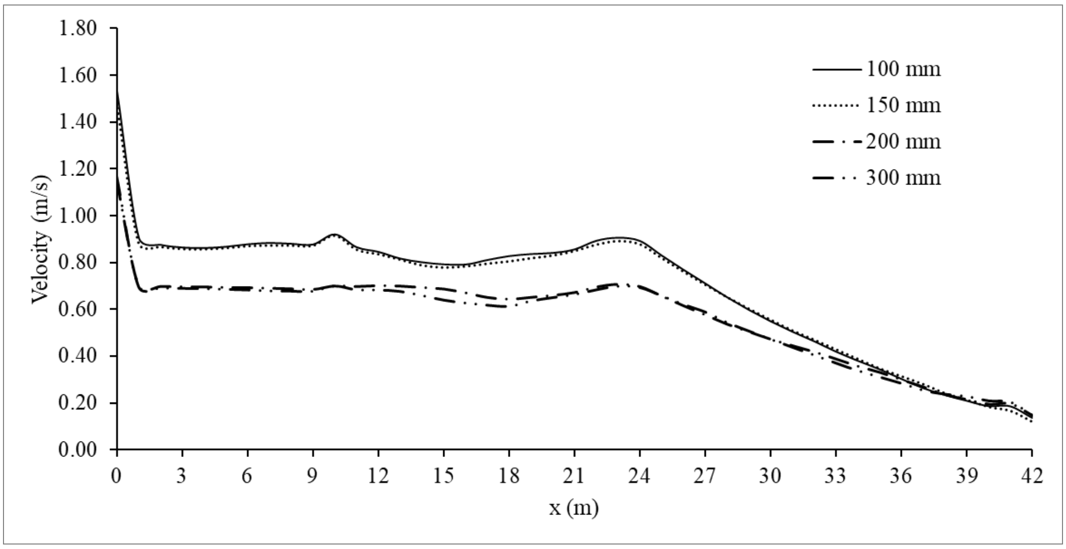

Figure 4. Average velocity of isosurfaces along x direction inside close house cage on various ECP

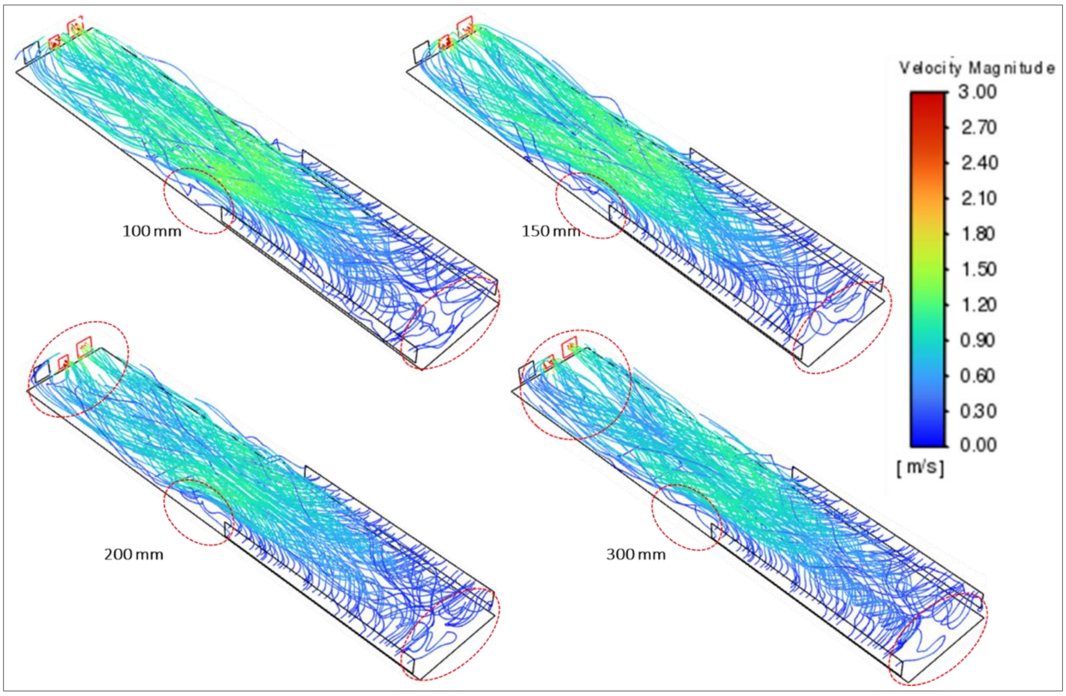

Figure 5. Velocity pathline of close house cage on various ECP thickness

The airflow patterns formed in the central region of the closed-house cage exhibit similar flow configuration characteristics. However, distinct differences in the fluid flow patterns are observed near the exhaust fan, indicated by the emergence of dead zones and damaging zones. The formation of these zones results from the interaction between internal vortices within the enclosure. Dead zones and damaging zones are identified based on the pathlines depicted in **Figure 5**. **Figure 5** illustrates the variations in pathline patterns within the closed-house cage corresponding to different ECP thicknesses of 100 mm, 150 mm, 200 mm, and 300 mm. The operational condition analyzed is designated as C 1-1-0, in which both the large and small exhaust fans are activated. Damaging zone only appear in front of the exhaust fan due to the suction process. While, the dead zone is indicated by the red line in **Figure 5**. Simulation results reveal the presence of wider dead zones in the 200 mm and 300 mm ECP configurations. These dead zones become more extensive due to the reduction in airflow velocity resulting from the increased ECP thickness. Additionally, dead zones consistently appear near the rear wall of the closed-house cage across all variations of ECP thickness.

Relative humidity within the closed-house cage is critical for determining livestock comfort. Figure 6a presents the graph of RH variation along the isosurface in the x-direction. In general, the influence of ECP thickness does not result in significant changes in the average RH trendline along the x-axis. The installation of a 100 mm ECP produces a higher RH compared to other variations. With the 100 mm ECP, the fluid flow velocity is higher than with the other ECP thicknesses. Consequently, a greater supply of fresh and humid air enters the room. As the air passes through, rapid heat exchange occurs. The water vapor carried by the fluid flow does not have sufficient time to evaporate completely, leading to a higher accumulation of humid air within the room. This condition will be further explained through the mass flow analysis in the subsequent subsection. In addition to the graphs, room humidity can also be mapped through RH contours. The centerline region of the closed-house cage exhibits higher RH compared to other areas. The centerline is the convergence area of the two large vortices formed within the cage. In this region, there is an accumulation of humid air due to the interaction of the two vortices. The RH contours of the airflow are illustrated in Figure 7a.

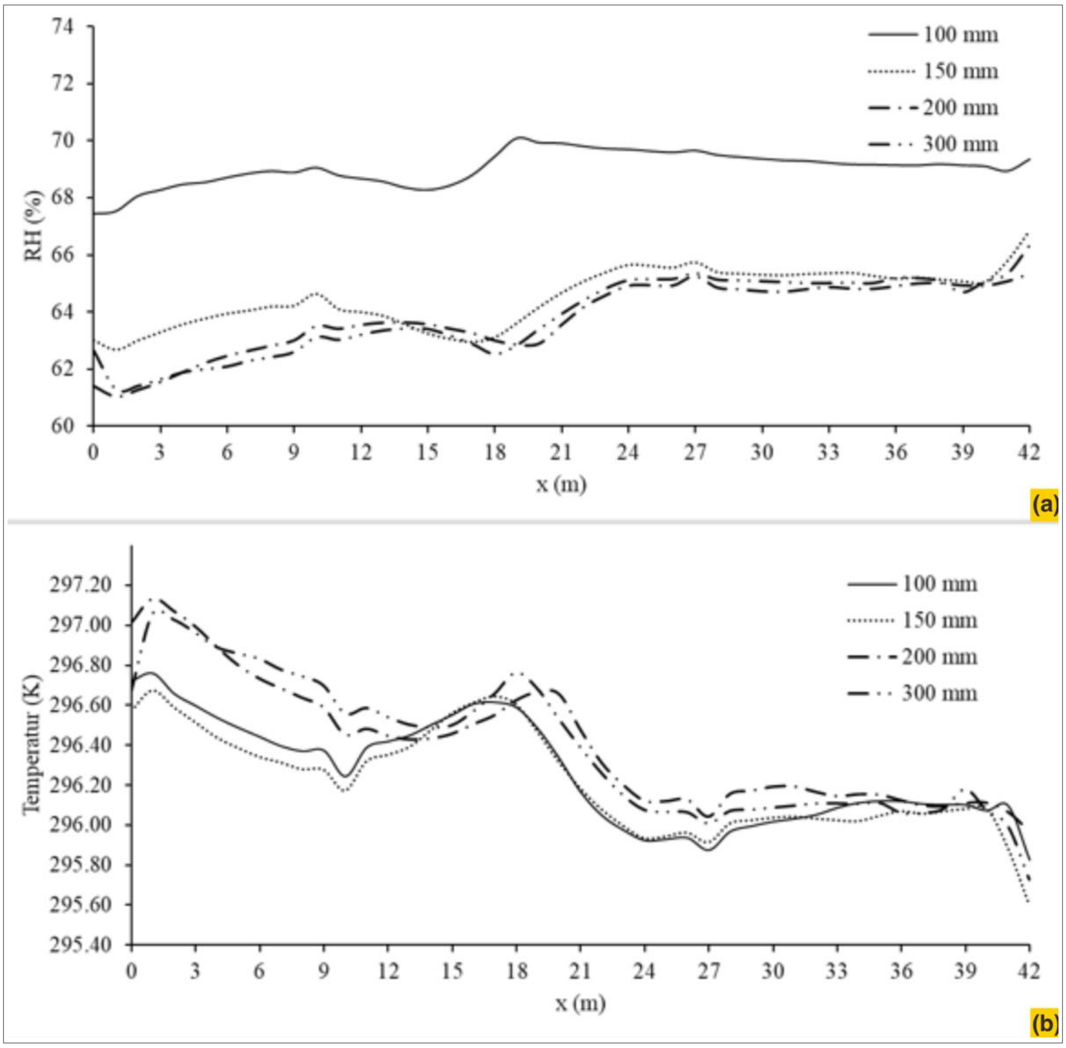

Figure 6. Graphics of average (a) RH and (b) temperatur of isosurfaces along x direction inside close house cage on various ECP thickness

The transformation of airflow patterns and velocities significantly influences the temperature distribution within the closed-house cage. Figure 6b illustrates the temperature distribution under the operational condition in which both a large and a small exhaust fan are activated. As depicted in Figure 6b, temperature variations are observed throughout the enclosure. The lowest air temperatures are concentrated near the ECP, where the influx of fresh air occurs. In general, the centerline region consistently exhibits the highest temperatures across all ECP installation scenarios. In this region, higher-velocity airflow along the side walls enhances accelerated heat transfer from the chickens, which serve as the primary heat source. This rapid heat transfer phenomenon results in a faster temperature increase at the center of the cage. Conversely, the airflow along the side walls maintains lower temperatures due to the effects of vortex circulation. The warmer, lower-density air near the chickens rises and circulates toward the roof. As the air moves closer to the exhaust fan, it carries thermal energy from the chickens, causing a further temperature increase. The installation of thinner ECPs facilitates a more rapid reduction in internal cage temperature. This trend is demonstrated by the graphs in **Figure 6b**, which present the average temperature values along the isosurface in the x-direction.

Ammonia (NH_3) and carbon dioxide (CO_2) are hazardous gases produced by chickens' respiration. In the high concentration the gases cause respiratory issues and high mortality. Effective HVAC systems can mitigate the accumulation of these hazardous gases (**Figure 8**). **Figure 9** presents the CO_2 gas distribution contours at various ECP thicknesses inside close house cage. High concentrations of CO_2 is illustrated in light blue color. Simulation results indicate that high levels of CO_2 accumulate predominantly in the centerline area, particularly at a height of 0.25 meters from

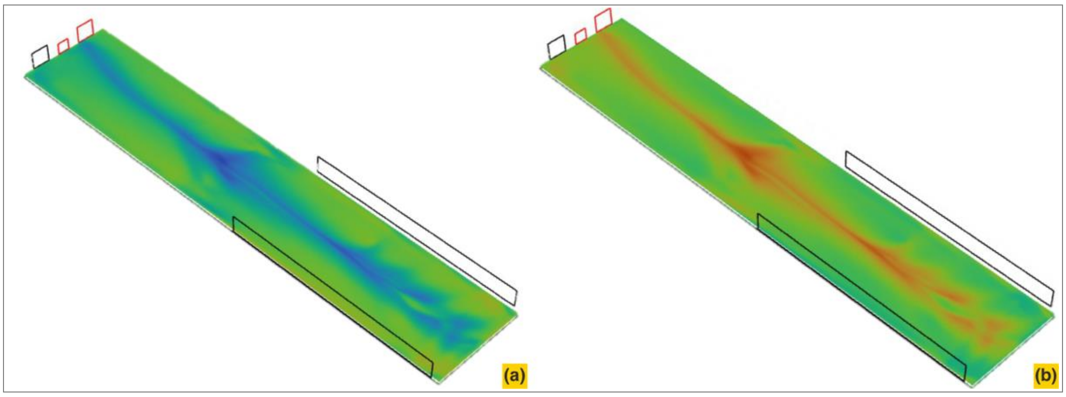

Figure 7. (a) Relative humidity and; (b) temperature contour y = 0.25 m in close house cage on various ECP thickness

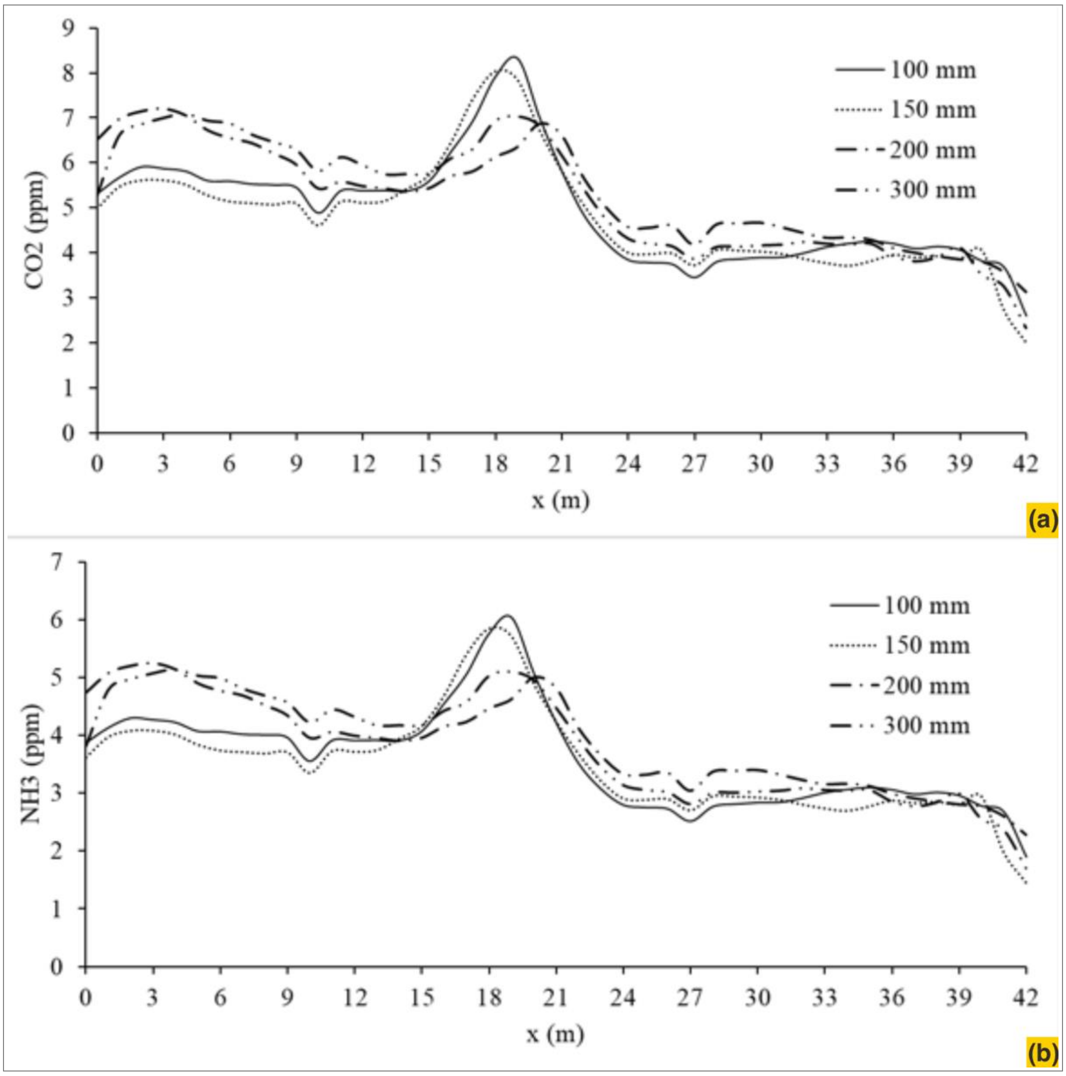

Figure 8. Average (a) CO_2 and; (b) NH_3 of isosurfaces along x direction inside close house cage on various ECP thickness

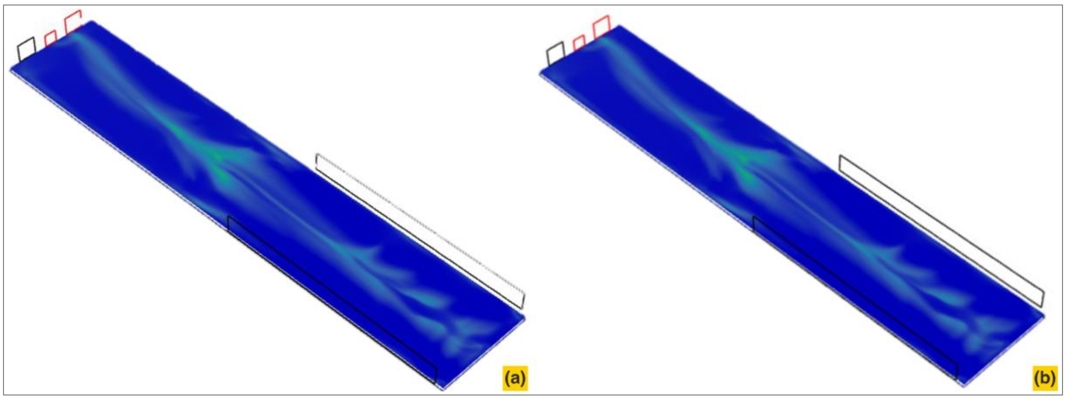

Figure 9. (a) CO_2 and; (b) NH_3 contour y = 0.25 m in close house cage on various ECP thickness

the floor. This region represents the air that the chickens inhale. The elevated CO_2 levels in the centerline area are due to low-speed airflow trapped between two large vortices, preventing the gas from rising with the warm air. As the airflow gradually exits the cage toward the exhaust fan, CO_2 accumulation decreases. The installation of a 300 mm thick ECP has higher concentration CO_2 accumulation area compared to other ECP thicknesses.

In addition to the formation of large vortices at the centerline of the cage, CO_2 gas also accumulates in the lower corner areas of the side walls of the closed house cage (**Figure 10**). The distribution of NH_3 gas inside the closed house cage is similar to that of CO_2, as illustrated in **Figure 11**. However, the concentration of NH_3 gas is lower than CO_2 levels. Farmers should monitor NH_3 accumulation on the side walls. NH_3 has several negative effects on chicken flock. These include respiratory disorders, reduced feed intake, diminished growth rates or egg production, lower feed conversion efficiency, increased vulnerability to infectious diseases, and higher mortality rates [38].

Accumulation of CO_2 gas in high levels directly affect blood pH, blood gases, and other circulating metabolites disruption [39]. **Figure 12** represent the maximum concentration of CO_2 and NH_3 level inside the closed house cage. The levels of CO_2 in **Figure 12a**, remain inside safe limits in all different thickness, as they are below 1000 ppm. Farmers also should monitor NH_3 accumulation inside the close house. In **Figure 12b** the accumulation of NH_3 in 150 mm is over the permissible limit 50 ppm than another variations. The highest NH_3 accumulation is located in the area near the exhaust fan at x = 18 m. The NH_3 accumulation in that area occurs due to indoor air alternatingly exiting the closed-house cage through the open exhaust. High level of NH_3 Elevated ammonia levels (e.g., exceeding 25 ppm) lead to decreased production efficiency and adverse effects on welfare and health. Maintaining cleanliness in the side wall areas is crucial to prevent mortality. In addition, farmers should try to keep livestock away from areas with NH_3 accumulation or speed up the airflow using additional HVAC systems, such as internal fan.

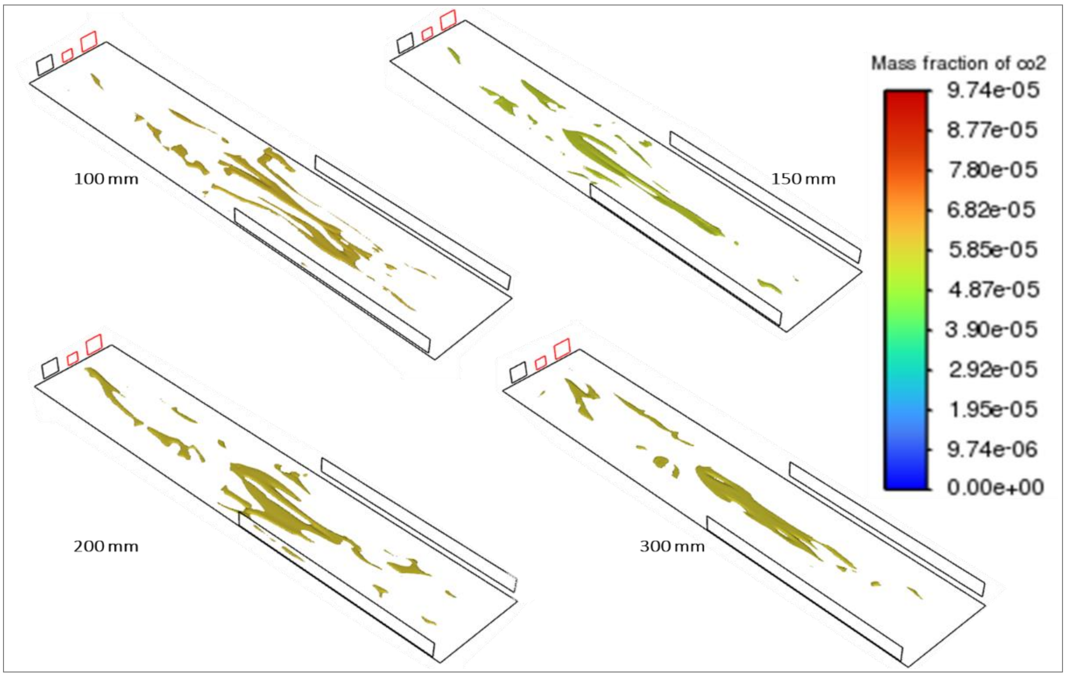

Figure 10. Accumulation CO_2 contour in close house cage on various ECP thickness

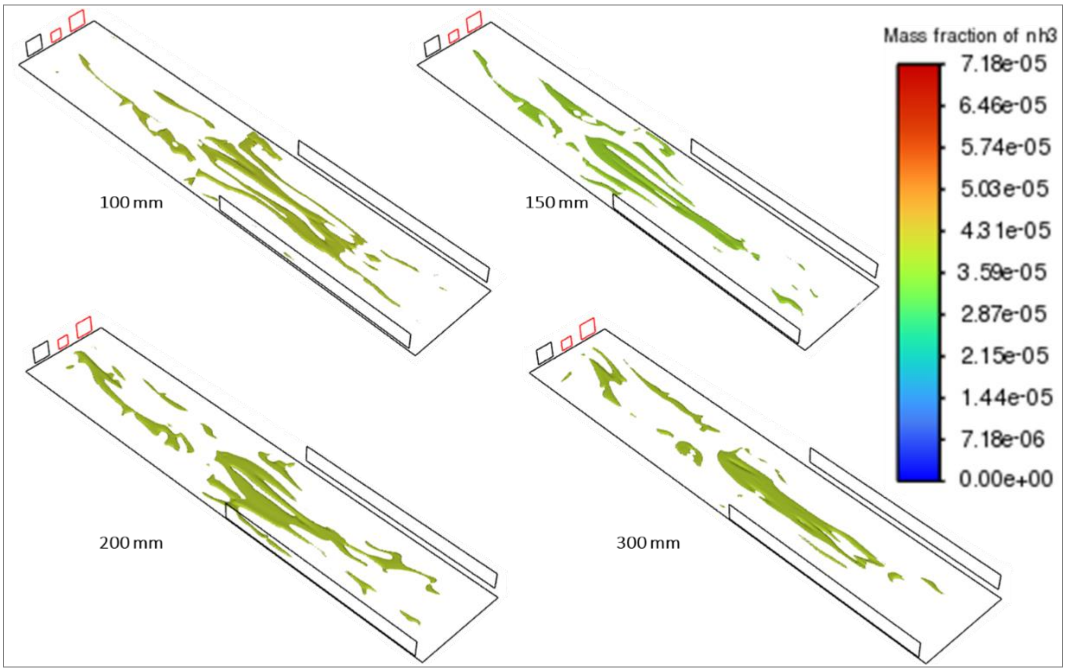

Figure 11. Accumulation NH_3 contour in close house cage on various ECP thickness

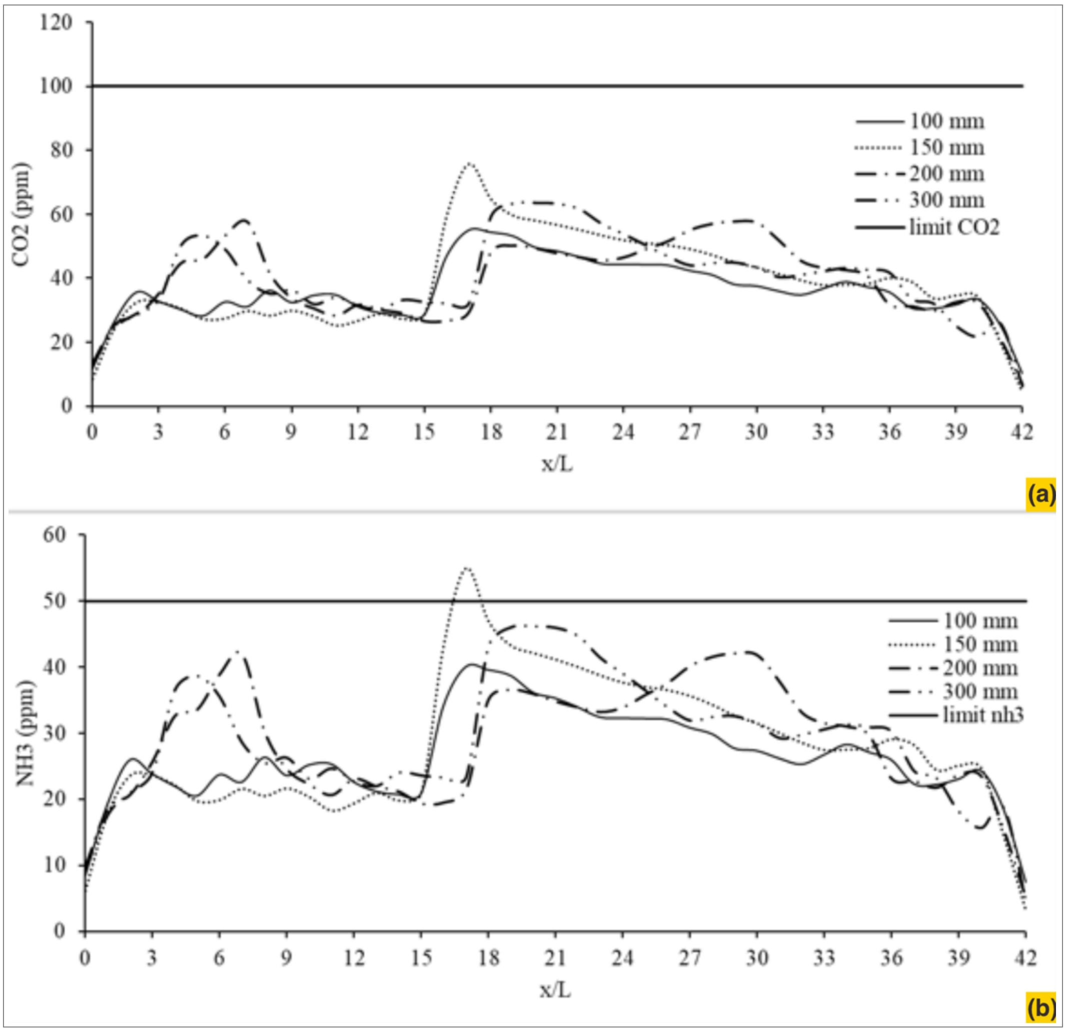

Figure 12. Maximum number of: (a) CO_2 and; (b) NH_3 on various ECP thickness in close house cage

2.3. The Effect of Exhaust Fan Operating Pattern

The variation in average fluid flow velocity within the closed-house cage is presented in **Figure 13**. The operation of a single exhaust fan under conditions C 1-0-0 and C 0-1-0 results in a more uniform distribution of average airflow velocity, as indicated by the flatter trendlines observed in the fluid velocity graphs. An increase in the number of active exhaust fans leads to a corresponding rise in airflow velocity within the closed-house cage. The highest average velocities are recorded in the front section of the cage, specifically within the range of x = 0–24 meters from the exhaust fan. As airflow approaches the exhaust fan, its velocity progressively increases. In contrast, the lowest flow velocities are observed in the rear section of the closed-house cage.

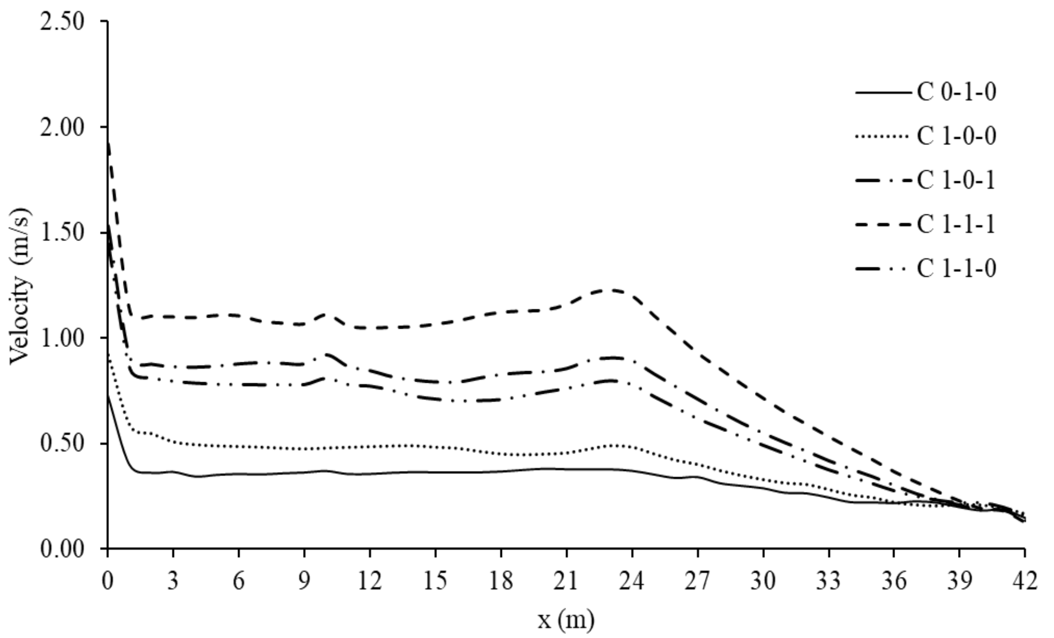

Figure 13. Average velocity of isosurfaces along x direction inside close house cage on exhaust opperating pattern

Fresh airflow entering through the ECPs on both the right and left sides collides and rolls into vortical structures. Two large vortices are consistently observed in the rear region of the cage across nearly all variations of exhaust fan operating patterns. As the airflow approaches the exhaust fans, the size of the vortices diminishes due to the separation of the fluid flow toward the open exhaust outlets. The internal airflow patterns within the closed-house cage are depicted through the pathlines illustrated in **Figure 14**. Dead zones consistently emerge in the rear section of the cage under nearly all exhaust fan operation scenarios. Moreover, the dead zone also emerge in the side wall after the air flow pass the ECP. Damaging zone only appear in front of the exhaust fan due to the suction process. While, the dead zone is indicated by the red line in **Figure 14**. The utilization of multiple exhaust fans effectively mitigates the extent of damaging zones within the closed-house cage. Higher-velocity airflow serves to minimize the formation of stagnant zones typically found in front of the exhaust fans.

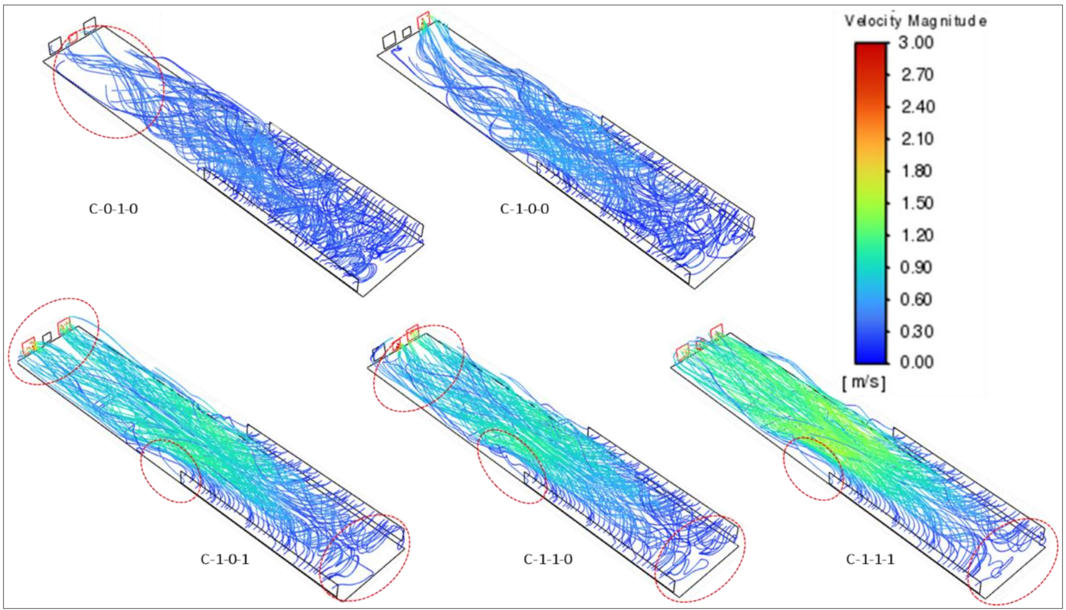

Figure 14. Velocity pathline of close house cage on various exhaust fan operating pattern

An increase in relative humidity (RH) within the closed-house cage can be achieved by operating multiple exhaust fans. This section presents a comparison of the effects of exhaust fan operation on air humidity levels in a closed-house cage equipped with a 200 mm ECP. The operation of a greater number of exhaust fans enhances the supply of fresh air with higher humidity content entering the enclosure. As a result, the increased mass flow rate of air leads to a corresponding rise in ambient humidity levels. Figure 15 illustrates the variation in RH along the isosurface in the x-direction, demonstrating that as the airflow approaches the exhaust fans—within the range of x = 0–15 meters—the relative humidity inside the enclosure decreases progressively.

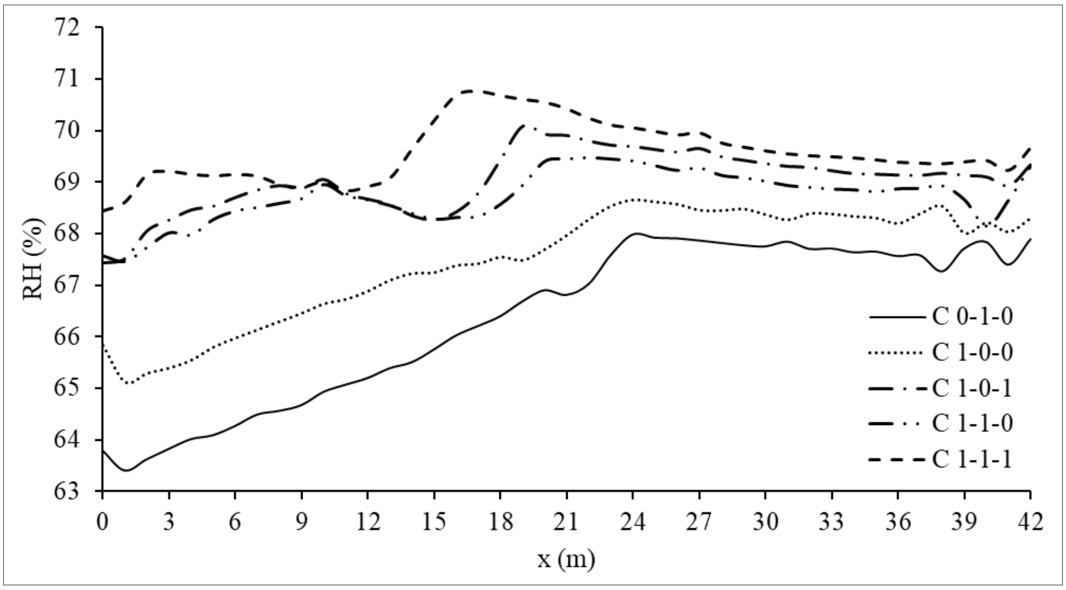

Figure 15. Average RH of isosurfaces along x direction inside close house cage on exhaust opperating pattern

The distribution of room humidity can be depicted through RH contours, as illustrated in Figure 16. The centerline region consistently exhibits higher humidity levels under various exhaust fan operation patterns. The operation of a single exhaust fan leads to a reduction in humidity levels near the exhaust fan area. This condition can be correlated with the presence of damaging zones, as depicted in the pathline visualizations. Damaging zones are characterized by regions with insufficient fresh air supply, resulting from low airflow velocity, which leads to inadequate air circulation within the enclosure.

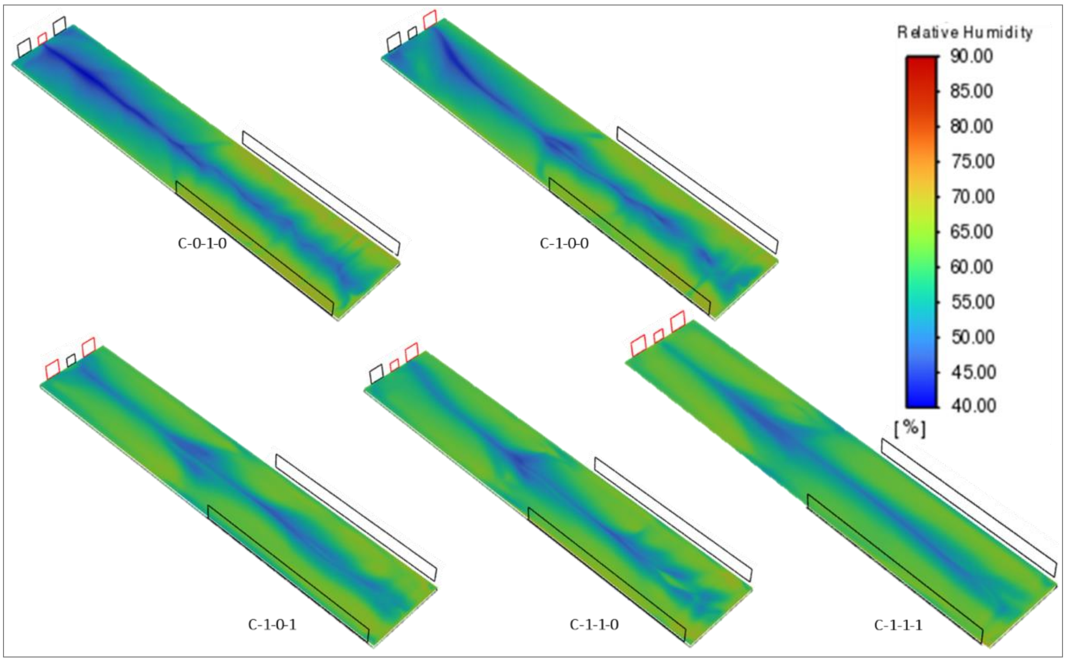

Figure 16. Relative humidity contour of close house cage on various exhaust fan operating pattern

The transformation of air flow velocity and pattern is affected by temperature distribution inside the closed house cage. The **Figure 17** illustrates temperature changes in the closed house cage with a 200 mm ECP thickness. The lowest air temperature is detected near the ECP, where fresh air enters. The area around the chickens has highest temperature across various exhaust fan operation patterns. The centerline area has the highest air flow velocity than sidewall area. The heat release from the chicken as the heat source in the centerline is more rapid. Therefore, the air flow in the centerline becomes warmer and has lower density. Meanwhile the temperature around the side walls has lower temperature, as the air circulates and forms a vortex. Meanwhile, in exhaust fan operation patterns C 0-1-0 and C 1-0-0, the velocity, which results in longer heat transfer process. Moreover, the operation of a single exhaust fan reduces the fresh air supply into the room.

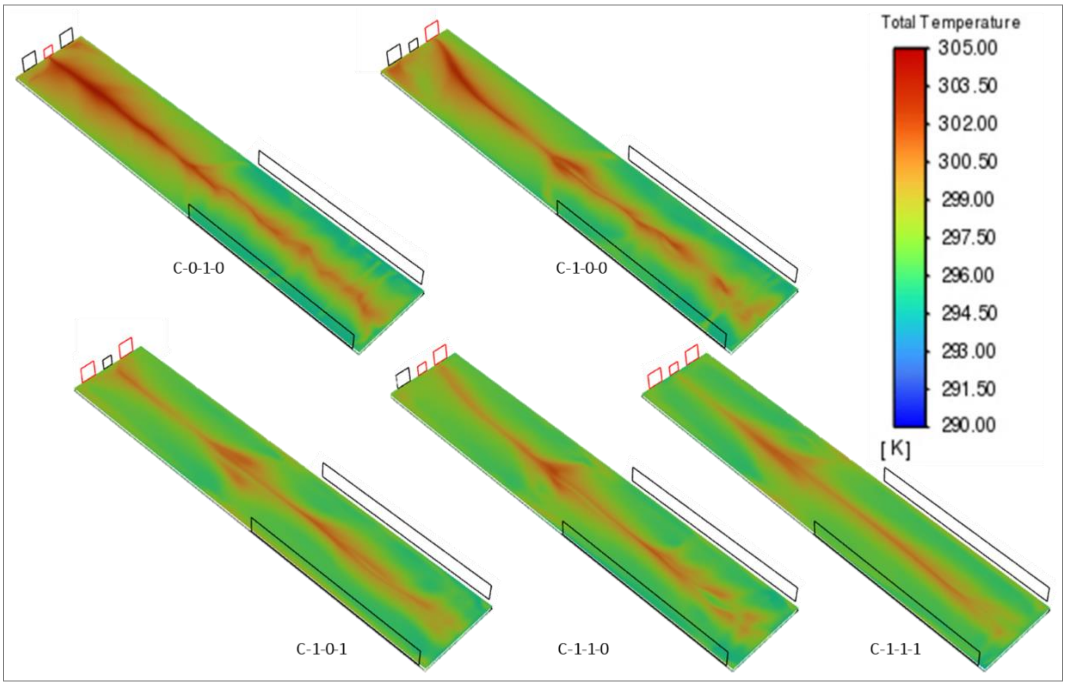

Figure 17. Temperatur contour of close house cage on various exhaust fan operating pattern

The contour mapping of fluid temperature distribution within the closed-house cage reveals results similar to those observed in the RH contours. However, the temperature graphs 18 exhibit an inverse correlation compared to the RH graphs. The graph plotted along the x-direction indicates that as the airflow approaches the exhaust fan (near point 0), the fluid temperature progressively increases. This occurs because the air near the exhaust fan has absorbed heat from the livestock and is in the process of exiting the closed-house cage. An analysis of both the RH contours (**Figure 16**) and the temperature contours (**Figure 17**) suggests that damaging zones induced by the operation of a single exhaust fan present a hazard to animal welfare. Elevated temperatures combined with low relative humidity levels may contribute to the onset of heat stress in the livestock.

Figure 19 presents the graph illustrating the influence of exhaust fan operation patterns on the maximum accumulation of CO_2 concentration along the isosurface in the x-direction within the closed-house cage. Overall, the highest CO_2 concentrations in the fluid flow are observed in the middle region of the closed-house cage, specifically between x = 12–24 meters. Simulation results demonstrate that single fan operation patterns, namely C 0-1-0 and C 1-0-0, yield a more fluctuating trendline for CO_2 accumulation. This behavior is characterized by the appearance of small wave patterns along the trendline of the average velocity graph (**Figure 18**). In contrast, the activated of multiple exhaust fans produces a more stable CO_2 accumulation trendline within the range of x = 15–39 meters. The presence of wave patterns in the graph may indicate fluid interactions, which can be further depicted and analyzed through flow pathline visualizations.

The pathlines in **Figure 14** illustrate the variations in airflow patterns resulting from different exhaust fan operation configurations. The closed-house cage is equipped with a 200 mm ECP and was simulated under five distinct operating scenarios. Fresh air entering through the ECPs on the right and left sides collides and rolls into vortical structures. Simulation results demonstrate that single fan operations, under both C 1-0-0 and C 0-1-0 configurations, generate rapidly swirling vortices, resulting in the formation of short-wave patterns. In contrast, the use of multiple exhaust fans produces fewer airflow wave patterns, with longer and more stable vortex swirls, particularly after passing through the ECPs. Higher CO_2 accumulation regions are observed under multiple fan operation patterns. Interestingly, single fan operation, characterized by shorter vortex swirls, facilitates faster transfer of CO_2 from the chickens into the surrounding air. However, single fan operation also contributes to CO_2 buildup in front of the exhaust fans. A reduced number of operating exhaust fans leads to significant CO_2 accumulation in the front section of the closed-house cage. This finding is consistent with the CO_2 accumulation contours depicted in **Figure 20**.

Proper placement of exhaust fans can mitigate the accumulation of these gases. **Figure 21** illustrates the distribution of CO_2 gas inside a closed house cage under various exhaust fan operating patterns. The contours shown in the figure represent areas where CO_2 accumulation exceeds 50 ppm, a level far below the established threshold of > 1000 ppm. The lowest concentration of CO_2 was observed in operating condition C 1-0-0, while the highest CO_2 accumulation occurred under operating condition C 0-1-0, followed by C 1-0-1, C 1-1-0, and C 1-1-1, respectively. Generally, CO_2 accumulation is concentrated near the center of the cage, close to the ECP. However, under the C 0-1-0 operating pattern, gas accumulation was observed near the exhaust fan, as the two large exhaust fans on the right and left sides were closed, allowing CO_2 to exit only intermittently through the smaller exhaust. Overall, none of the exhaust fan operating patterns resulted in CO_2 accumulation above the threshold. The C 1-1-1 operating condition produced the highest CO_2 levels in rare area of close house cage, indicating that CO_2 carried by airflow entered the vortex and accumulated at the center of the closed house cage.

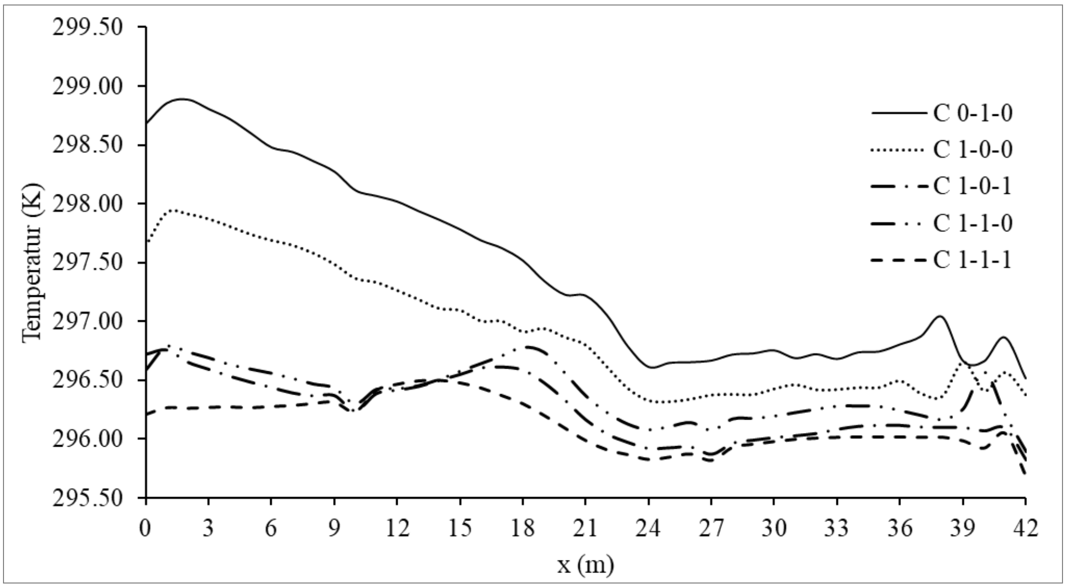

Figure 18. Average temperature of isosurfaces along x direction inside close house cage on exhaust opperating pattern

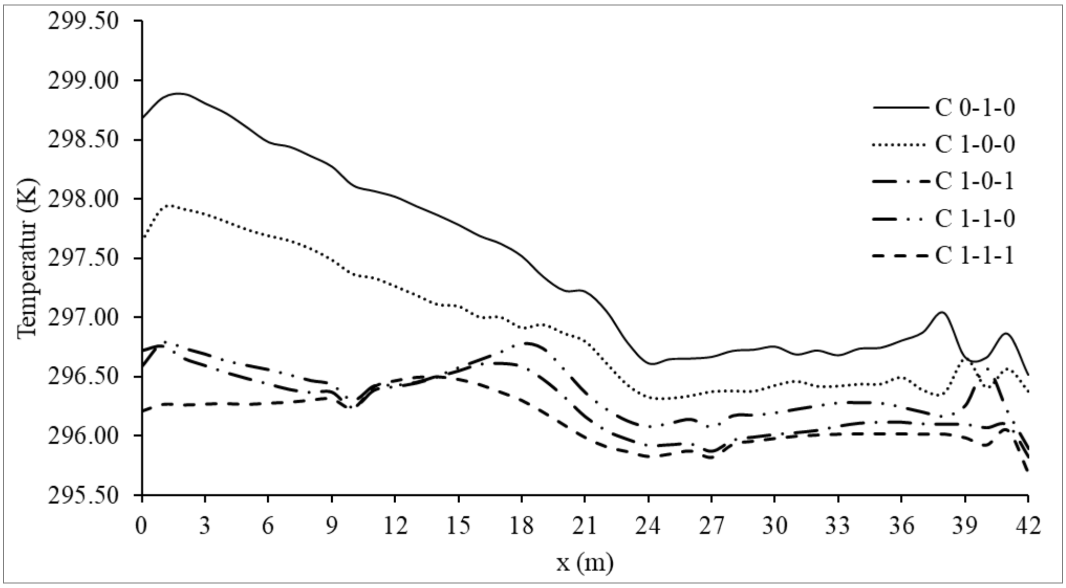

Figure 19. Maximum accumulation CO_2 of isosurfaces along x direction inside close house cage on exhaust opperating pattern

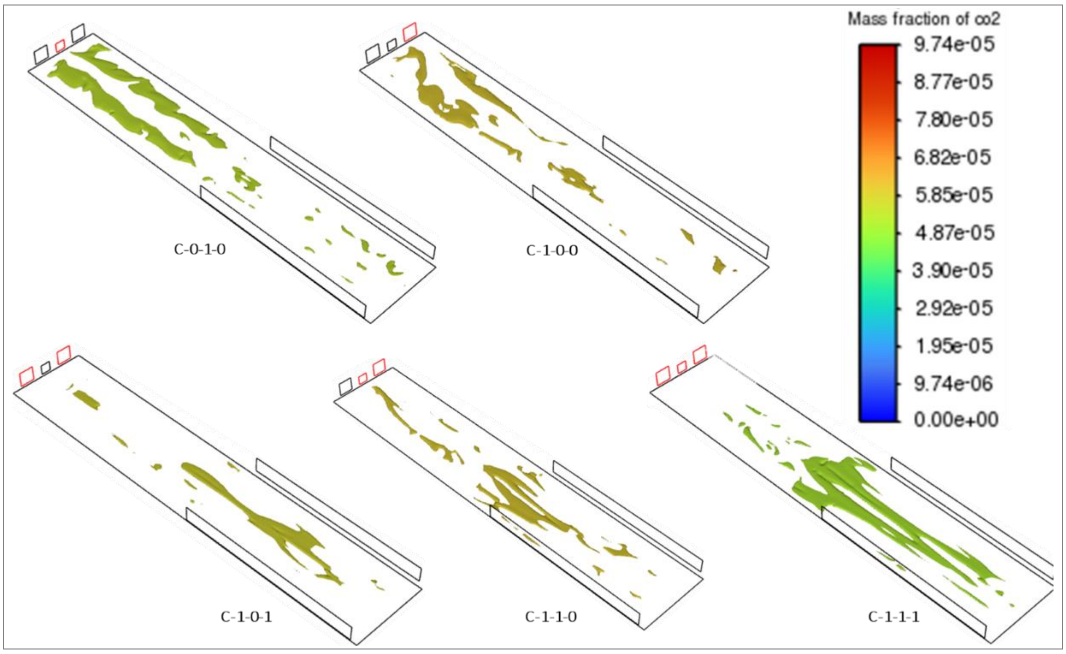

Figure 20. Accumulation CO_2 contour in close house cage on various exhaust fan operating pattern

NH_3 gas distribution has similar pattern as CO_2. **Figure 21** shows NH_3 accumulation exceeding 25 ppm inside the closed house cage. The operating pattern C 0-1-0 has the highest NH_3 accumulation compared to other patterns, differing significantly from the CO_2 accumulation observed in the previous section. NH_3 has a higher density than CO_2, which allows it to accumulate more easily near the chickens, unlike CO_2, which is lighter and more readily carried by airflow. As the NH_3 layer inside the cage thickens, the CO_2 layer rises, making it more susceptible to displacement by higher-velocity fluid flow. The single operating patterns, C 1-0-0, have second ranks NH_3 accumulation, followed by multiple operating exhaust fan C 1-0-1, C 1-1-0 and C 1-1-1. Activating all exhaust fans does not yield a significant improvement in air quality for the closed house cage due to the formation of a stronger vortex. NH_3 can cause metabolic disruptions and mortality in chickens. Various studies recommend different NH_3 accumulation thresholds, ranging from >25 ppm to 50 ppm and 100 ppm. Therefore, it is advisable for poultry farmers to use exhaust fans with higher pressure or increase the number of fans in operation, as seen in another operating patterns.

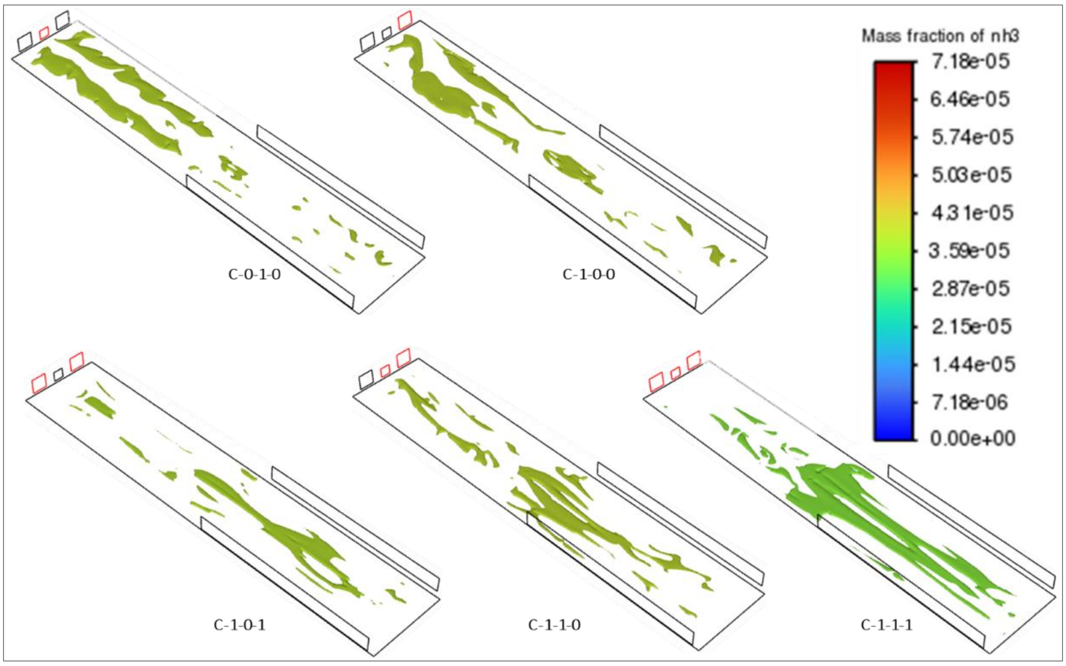

Figure 21. Accumulation NH_3 contour in close house cage on various exhaust fan operating pattern

The graphs of maximum hazardous gas accumulation (**Figure 21**) and average hazardous gas accumulation (**Figure 22**) exhibit distinct distribution patterns, indicating a non-uniform dispersion of hazardous gases within the closed-house cage. In particular, the front area of the cage, located near the exhaust fans and farther from the ECP, demonstrates a high average hazardous gas accumulation (Figure 22), while the maximum accumulation value in this region remains lower compared to that observed along the centerline. This suggests that hazardous gas accumulation in the frontal area, although at elevated concentrations, covers a broader spatial region. Conversely, in the centerline region, the maximum accumulation values are higher, but the average accumulation remains relatively low. This indicates that hazardous gases with high concentrations near the centerline are confined to a narrower area, predominantly near the roof, despite exhibiting significantly high localized accumulation levels.

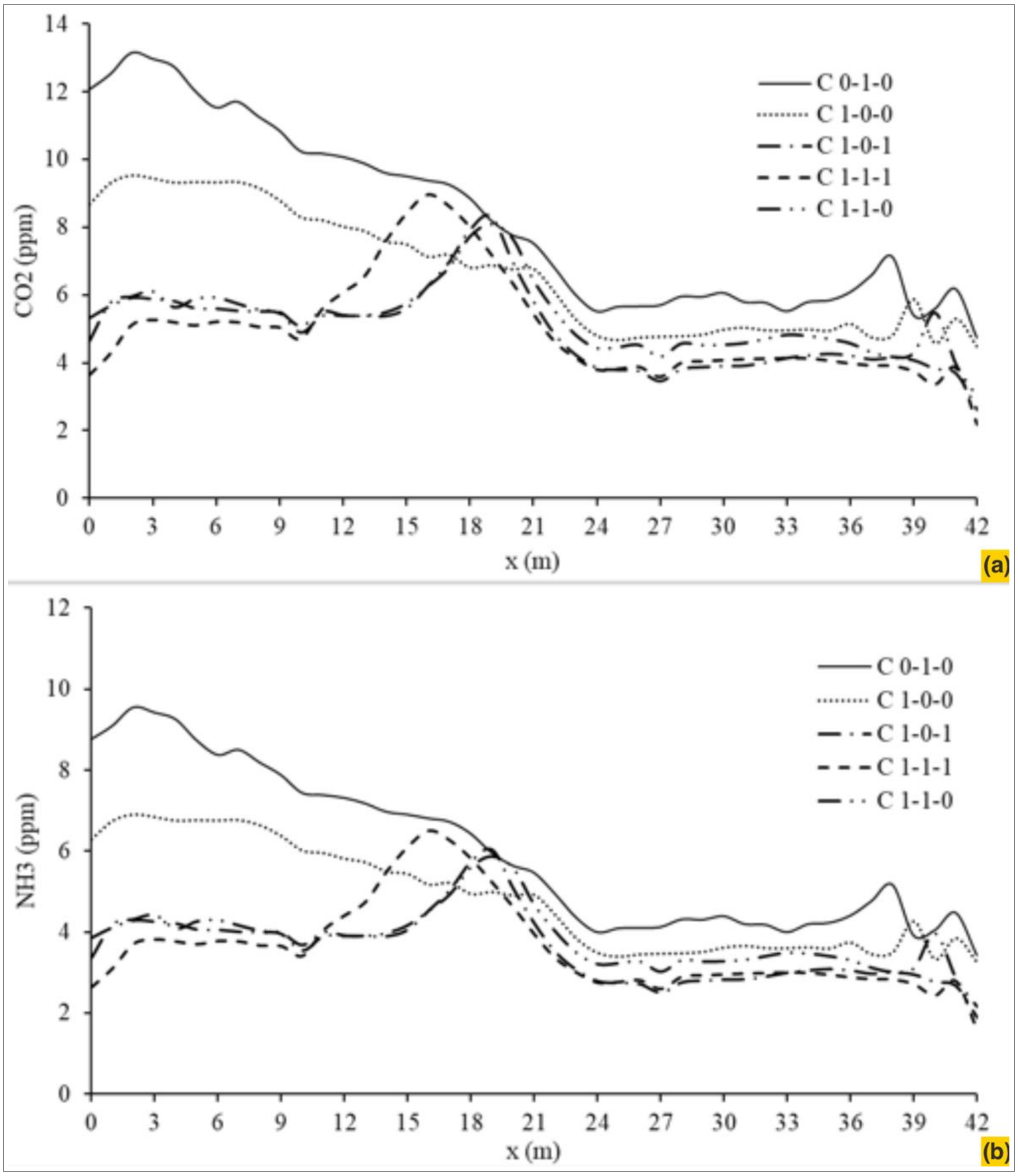

Figure 22. Average number of: (a) CO_2 and; (b) NH_3 on various exhaust fan operating pattern

2.4. Overview of Exhaust Fan Operating Pattern and ECP Thickness Effect

This section provides a summary of the variations in the effects of ECP installation and exhaust fan operation patterns. It is important to recognize that the combination of different operating patterns and ECP thicknesses results in variations in the mass flow rate of fresh air supplied to the closed-house cage. An increased supply of fresh air enhances heat transfer between the livestock and the mass flow rate, as illustrated in Figure 23b and Figure 23a. The operation of multiple exhaust fans in a closed-house cage equipped with thinner ECPs enhances more rapid heat transfer, driven by the increased supply of fresh air.

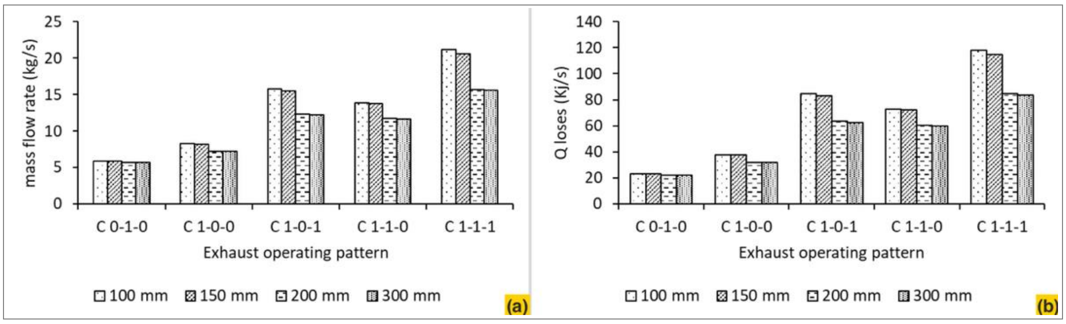

Figure 23. (a) fresh air mass flow and; (b) Q heat transfer in various ECP thickness and exhaust dan operating pattern

A high mass flow rate of fresh air alone is insufficient to achieve optimal and comfortable conditions for livestock. **Figure 24** illustrates the hazardous conditions at the iso-surfaces along the x-direction within the closed-house cage. In addition to fresh air supply, parameters such as temperature, relative humidity (RH), and hazardous gas accumulation are employed to evaluate the effectiveness of different exhaust fan operation patterns and ECP thicknesses. The assessment criteria are based on velocity exceeding 2 m/s, temperature greater than 298 K, RH maintained between 60% and 80%, CO_2 concentrations exceeding 1000 ppm, and NH_3 concentrations greater than 50 ppm on the iso-surfaces. The values for velocity, RH, CO_2, and NH_3 are derived from the maximum values across 42 iso-surfaces, each spaced 1 meter apart. This study demonstrates that a 100 mm thick ECP results in a lower extent of danger zones across all exhaust fan operation patterns. Furthermore, exhaust fan operation patterns C 1-0-0, C 1-0-1, and C 1-1-0 exhibit fewer danger zones compared to patterns C 1-1-1 and C 0-1-0. These findings indicate that operating three exhaust fans simultaneously does not necessarily improve environmental conditions within the closed-house poultry cage.

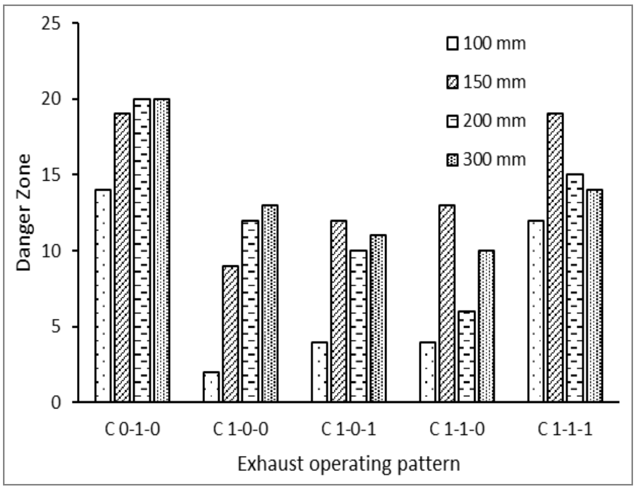

Figure 24. Total dangerous zone in various ECP thickness and exhaust dan operating pattern

3. Conclusion

Based on the results of numerical simulation with various variation in ECP thickness and Exhaust fan operation pattern, it can be concluded as follows:

a. A humid and cool environment is necessary for the cultivation of broiler poultry in this ideal environment. The installation of an ECP leads to a more consistent airflow, which is characterized by increased humidity and reduced temperatures. A higher pressure drop is the consequence of a thicker ECP, which leads to a slower passage of fresh air. The reduction of the fresh air supply results in an increase in temperatures and an accumulation of hazardous gases. In comparison to other ECP thickness variations, the thinnest ECP (100 mm) generates a smaller number of hazardous locations.

b. The momentum of the air entering the confined house cage is increased when the exhaust fan is fully operational. This condition is not optimal because it not only increases energy consumption but also increases the turbulence of fluid flow within the confined house cage. Even with an increased air supply, the C 1-1-1 operation pattern creates a more hazardous environment for the poultry.

Acknowledgements

The authors are grateful to Kementerian Pendidikan, Kebudayaan, Riset, dan Teknologi (Center for Higher Education Funding-BPPT), Pusat Pembiayaan dan Asesmen Pendidikan Tinggi (PPAPT) and Lembaga Pengelola Dana Pendidikan (LPDP) for supporting this research. The author is grateful for the time and support provided by Vivien Suphandani Djanali, S.T., M.Eng., Ph.D., for the discussion. The author also express gratitude to the editor and reviewers for their valuable contributions in refining up this manuscript.

Authors' Declaration

Authors' contributions and responsibilities - The authors made substantial contributions to the conception and design of the study. The authors took responsibility for data analysis, interpretation and discussion of results. The authors read and approved the final manuscript.

Funding – No funding information from the authors.

Availability of data and materials - All data is available from the authors.

Competing interests - The authors declare no competing interests.

Additional information – No additional information from the authors.

References

[1] S. Al-Benna, "Negative pressure rooms and COVID-19," *Journal of Perioperative Practice*, vol. 31, no. 1–2, pp. 18–23, Jan. 2021, doi: 10.1177/1750458920949453.

[2] K. Ahmadi Babadi, H. Khorasanizadeh, and A. Aghaei, "CFD modeling of air flow, humidity, CO2 and NH3 distributions in a caged laying hen house with tunnel ventilation system," *Computers and Electronics in Agriculture*, vol. 193, p. 106677, Feb. 2022, doi: 10.1016/j.compag.2021.106677.

[3] Ilda De Fatima Ferreira Tinoco, Jairo Alexander Osorio, Flavio Alves Damasceno, Richard S Gates, Keller Sullivan Rocha, and Olga Lucia Zapata, "3D-CFD Modeling of a Typical Uninsulated and Internal Misting Tunnel Ventilated Brazilian Poultry House," in *2010 Pittsburgh, Pennsylvania, June 20 - June 23, 2010*, St. Joseph, MI: American Society of Agricultural and Biological Engineers, 2010, p. 1. doi: 10.13031/2013.29817.

[4] E. Küçüktopcu, B. Cemek, H. Simsek, and J.-Q. Ni, "Computational Fluid Dynamics Modeling of a Broiler House Microclimate in Summer and Winter," *Animals*, vol. 12, no. 7, p. 867, Mar. 2022, doi: 10.3390/ani12070867.

[5] K. Shahzad *et al.*, "Experiments on Energy-Efficient Evaporative Cooling Systems for Poultry Farm Application in Multan (Pakistan)," *Sustainability*, vol. 13, no. 5, p. 2836, Mar. 2021, doi: 10.3390/su13052836.

[6] M. P. dos Santos *et al.*, "Efficiency of cooling systems in broiler houses during hot days," *Ciência Rural*, vol. 51, no. 8, 2021, doi: 10.1590/0103-8478cr20200941.

[7] M. Munadi, M. N. Setiawan, A. H. Fauzi, A. Goni, I. Haryanto, and N. Iskandar, "Study of Sensor Placement and Temperature Control Reference Value Based on Computational Fluid Dynamics in Closed-Type Broiler Chicken Cage," in *2022 9th International Conference on Information Technology, Computer, and Electrical Engineering (ICITACEE)*, IEEE, Aug. 2022, pp. 90–95. doi: 10.1109/ICITACEE55701.2022.9923960.

[8] V. Chandra, N. Singh, S. Sharma, and M. Karnani, "Comparative efficacy of evaporative cooling pad and fogger system on behaviour of broiler chicken," *Indian Journal of Poultry Science*, vol. 57, no. 2, pp. 165–170, 2022, doi: 10.5958/0974-8180.2022.00030.7.

[9] A. Çaylı, A. Akyüz, S. Üstün, and B. Yeter, "Efficiency of two different types of evaporative cooling systems in broiler houses in Eastern Mediterranean climate conditions," *Thermal Science and Engineering Progress*, vol. 22, p. 100844, May 2021, doi: 10.1016/j.tsep.2021.100844.

[10] M. W. Dunlop and J. McAuley, "Direct surface wetting sprinkler system to reduce the use of evaporative cooling pads in meat chicken production: indoor thermal environment, water usage, litter moisture content, live market weights, and mortalities," *Poultry Science*, vol. 100, no. 5, p. 101078, May 2021, doi: 10.1016/j.psj.2021.101078.

[11] J. Lv, H. Xu, M. Zhu, Y. Dai, H. Liu, and Z. Li, "The performance and model of porous materials in the indirect evaporative cooling system: A review," *Journal of Building Engineering*, vol. 41, p. 102741, Sep. 2021, doi: 10.1016/j.jobe.2021.102741.

[12] A. Laknizi, M. Mahdaoui, A. Ben Abdellah, K. Anoune, M. Bakhouya, and H. Ezbakhe,

"Performance analysis and optimal parameters of a direct evaporative pad cooling system under the climate conditions of Morocco," *Case Studies in Thermal Engineering*, vol. 13, p. 100362, Mar. 2019, doi: 10.1016/j.csite.2018.11.013.

[13] P. A. Gonzalez-Rivas, S. S. Chauhan, M. Ha, N. Fegan, F. R. Dunshea, and R. D. Warner, "Effects of heat stress on animal physiology, metabolism, and meat quality: A review," *Meat Science*, vol. 162, p. 108025, Apr. 2020, doi: 10.1016/j.meatsci.2019.108025.

[14] A. Soliman and A. M. Safwat, "Climate Change Impact on Immune Status and Productivity of Poultry as Well as the Quality of Meat and Egg Products," in *Springer Water*, 2020, pp. 481–498. doi: 10.1007/978-3-030-41629-4_20.

[15] M. S. Ghoname, "Effect of pad water flow rate on evaporative cooling system efficiency in laying hen housing," *Journal of Agricultural Engineering*, vol. 51, no. 4, pp. 209–219, Dec. 2020, doi: 10.4081/jae.2020.1051.

[16] J. P. Harrouz, D. Al Assaad, M. Orabi, K. Ghali, D. Ouahrani, and N. Ghaddar, "Modeling and optimization of poultry house passive cooling strategies in semiarid climates," *International Journal of Energy Research*, vol. 45, no. 15, pp. 20795–20811, Dec. 2021, doi: 10.1002/er.7139.

[17] A. Franco, D. L. Valera, A. Peña, and A. M. Pérez, "Aerodynamic analysis and CFD simulation of several cellulose evaporative cooling pads used in Mediterranean greenhouses," *Computers and Electronics in Agriculture*, vol. 76, no. 2, pp. 218–230, May 2011, doi: 10.1016/j.compag.2011.01.019.

[18] T. O. Ahmadu, Y. S. Sanusi, and F. Usman, "Experimental evaluation of a modified direct evaporative cooling system combining luffa fiber—charcoal cooling pad and activated carbon dehumidifying pad," *Journal of Engineering and Applied Science*, vol. 69, no. 1, p. 63, Dec. 2022, doi: 10.1186/s44147-022-00116-1.

[19] F. A. Obando Vega, A. P. Montoya Rios, J. A. Osorio Saraz, F. A. Damasceno, and M. Barbari, "Comparative Analysis of the Cooling Efficiency in Tropical Climate of Three Alternative Materials for Evaporative Cooling Pads," *Applied Sciences*, vol. 12, no. 1, p. 77, Dec. 2021, doi: 10.3390/app12010077.

[20] M. S. Rahman, S. MacPherson, and M. Lefsrud, "Experimental investigation of a novel evaporative cooling pad made of cement-free porous concrete," *Building and Environment*, vol. 228, p. 109867, Jan. 2023, doi: 10.1016/j.buildenv.2022.109867.

[21] S. Suranjan Salins, S. V. K. Reddy, and S. Kumar, "Experimental investigation on use of alternative innovative materials for sustainable cooling applications," *International Journal of Sustainable Engineering*, vol. 14, no. 5, pp. 1207–1217, Sep. 2021, doi: 10.1080/19397038.2021.1924894.

[22] S. Abdel-Rahman, "Performance evaluation of poultry houses under different evaporative cooling systems," *Zagazig Journal of Agricultural Research*, vol. 47, no. 4, pp. 999–1010, Aug. 2020, doi: 10.21608/zjar.2020.110328.

[23] T. D. Nguyen and H. M. Bui, "Computational fluid dynamic model for smoke control of building basement," *Case Studies in Chemical and Environmental Engineering*, vol. 7, p. 100318, Jun. 2023, doi: 10.1016/j.cscee.2023.100318.

[24] A. Jahanbin, "Efficacy of coupling heat recovery ventilation and fan coil systems in improving the indoor air quality and thermal comfort condition," *Energy and Built Environment*, vol. 3, no. 4, pp. 478–495, Oct. 2022, doi: 10.1016/j.enbenv.2021.05.005.

[25] X. Tong, S.-W. Hong, and L. Zhao, "CFD modelling of airflow pattern and thermal environment in a commercial manure-belt layer house with tunnel ventilation," *Biosystems Engineering*, vol. 178, pp. 275–293, Feb. 2019, doi: 10.1016/j.biosystemseng.2018.08.008.

[26] X. Hui, "Effect of cooling pad installation on indoor airflow distribution in a tunnel-ventilated laying-hen house," *International Journal of Agricultural and Biological Engineering*, vol. 9, no. 4, pp. 169–177, 2016, doi: 10.3965/j.ijabe.20160904.2447.

[27] Xiaoshuai Wang and Kaiying Wang, "Optimizing the Pad Cooling Ventilation System of Laying Hen Barn Using CFD in Southeast China," in *2013 Kansas City, Missouri, July 21 - July 24, 2013*, St. Joseph, MI: American Society of Agricultural and Biological Engineers, 2013. doi: 10.13031/aim.20131620039.

[28] F. Rojano, P.-E. Bournet, M. Hassouna, P. Robin, M. Kacira, and C. Y. Choi, "Computational

modelling of thermal and humidity gradients for a naturally ventilated poultry house," *Biosystems Engineering*, vol. 151, pp. 273–285, Nov. 2016, doi: 10.1016/j.biosystemseng.2016.09.012.

[29] E. Bustamante, S. Calvet, F. Estellés, A. G. Torres, and A. Hospitaler, "Measurement and numerical simulation of single-sided mechanical ventilation in broiler houses," *Biosystems Engineering*, vol. 160, pp. 55–68, Aug. 2017, doi: 10.1016/j.biosystemseng.2017.05.009.

[30] L. Du *et al.*, "Computational Fluid Dynamics aided investigation and optimization of a tunnel-ventilated poultry house in China," *Computers and Electronics in Agriculture*, vol. 159, pp. 1–15, Apr. 2019, doi: 10.1016/j.compag.2019.02.020.

[31] H. Ma, Y. Tu, X. Yang, Z. Yang, and C. Liang, "Influence of tunnel ventilation on the indoor thermal environment of a poultry building in winter," *Building and Environment*, vol. 223, p. 109448, Sep. 2022, doi: 10.1016/j.buildenv.2022.109448.

[32] L. Rong, D. Liu, E. F. Pedersen, and G. Zhang, "The effect of wind speed and direction and surrounding maize on hybrid ventilation in a dairy cow building in Denmark," *Energy and Buildings*, vol. 86, pp. 25–34, Jan. 2015, doi: 10.1016/j.enbuild.2014.10.016.

[33] A. Franco, D. L. Valera, A. Madueño, and A. Peña, "Influence of Water and Air Flow on the Performance of Cellulose Evaporative Cooling Pads Used in Mediterranean Greenhouses," *Trans ASABE*, vol. 53, no. 2, pp. 565–576, 2010, doi: 10.1031/2013.29571.

[34] Q. Cheng, W. Wu, H. Li, G. Zhang, and B. Li, "CFD study of the influence of laying hen geometry, distribution and weight on airflow resistance," *Computers and Electronics in Agriculture*, vol. 144, pp. 181–189, Jan. 2018, doi: 10.1016/j.compag.2017.12.003.

[35] Q. Cheng, H. Feng, H. Meng, and H. Zhou, "CFD study of the effect of inlet position and flap on the airflow and temperature in a laying hen house in summer," *Biosystems Engineering*, vol. 203, pp. 109–123, Mar. 2021, doi: 10.1016/j.biosystemseng.2021.01.009.

[36] D. Fidaros, C. Baxevanou, T. Bartzanas, and C. Kittas, "Numerical study of mechanically ventilated broiler house equipped with evaporative pads," *Computers and Electronics in Agriculture*, vol. 149, pp. 101–109, Jun. 2018, doi: 10.1016/j.compag.2017.10.016.

[37] M. Fourar, G. Radilla, R. Lenormand, and C. Moyne, "On the non-linear behavior of a laminar single-phase flow through two and three-dimensional porous media," *Advances in Water Resources*, vol. 27, no. 6, pp. 669–677, Jun. 2004, doi: 10.1016/j.advwatres.2004.02.021.

[38] R. B. Bist, S. Subedi, L. Chai, and X. Yang, "Ammonia emissions, impacts, and mitigation strategies for poultry production: A critical review," *Journal of Environmental Management*, vol. 328, p. 116919, Feb. 2023, doi: 10.1016/j.jenvman.2022.116919.

[39] R. C. Beckford *et al.*, "Effects of heat stress on performance, blood chemistry, and hypothalamic and pituitary mRNA expression in broiler chickens," *Poultry Science*, vol. 99, no. 12, pp. 6317–6325, Dec. 2020, doi: 10.1016/j.psj.2020.09.052.

[40] E. Bustamante, F.-J. García-Diego, S. Calvet, A. Torres, and A. Hospitaler, "Measurement and Numerical Simulation of Air Velocity in a Tunnel-Ventilated Broiler House," *Sustainability*, vol. 7, no. 2, pp. 2066–2085, Feb. 2015, doi: 10.3390/su7022066.

[41] O. Ecim-Djuric and G. Topisirovic, "Energy efficiency optimization of combined ventilation systems in livestock buildings," *Energy and Buildings*, vol. 42, no. 8, pp. 1165–1171, Aug. 2010, doi: 10.1016/j.enbuild.2009.10.035.